İSTANBUL UNIVERSITY PRESS

COMPARISON OF PERFORMANCE CHARACTERISTICS OF GAMMA CAMERAS WITH SCINTILLATION NaI(TI) AND SEMICONDUCTOR CdZnTe DETECTORS

NaI(TI) SİNTİLASYON VE CdZnTe YARI İLETKEN DEDEKTÖRLÜ GAMA KAMERALARIN PERFORMANS ÖZELLİKLERİNİN KARŞILAŞTIRILMASI

Armağan AYDIN[1,3] ⓘ**, Füsun ÇETİN[2]** ⓘ**, Mustafa DEMİR[1,3]** ⓘ

[1]İstanbul University-Cerrahpaşa, Institute of Graduate Studies, Health Physics PhD Program, İstanbul, Türkiye
[2]İstanbul Aydın University, Institute of Health Sciences, Department of Health Physics, İstanbul, Türkiye
[3]İstanbul University-Cerrahpaşa, Cerrahpaşa Faculty of Medicine, Department of Nuclear Medicine, İstanbul, Türkiye

ORCID ID: A.A. 0000-0002-9126-8381; F.Ç. 0000-0001-9135-2615; M.D. 0000-0002-9813-1628

ABSTRACT

Objective: In recent years, gamma cameras with semiconductor detectors (CdZnTe) have entered routine practise diagnostic scintigraphic imaging in nuclear medicine. In this study, we aimed to compare the performance characteristics of a gamma camera with a semiconductor detector (CdZnTe) and a conventional gamma camera with a NaI(Tl) detector.

Material and Methods: In our experimental studies, spatial resolution, energy resolution, and linearity tests were performed using 3 capillary tubes of the same length and thickness, into which the Tc-99m radioisotope with different activities was placed. Sensitivity tests were performed by placing Tc-99m in a plastic Petri dish with a diameter of 3 cm. Scintigraphic images of the capillary tubes and the Petri dish were taken with both gamma cameras under equal geometric conditions. Regions of interest (ROI) were drawn on the images. The activity amount corresponding to the counts in the ROI was determined.

Results: The spatial resolution, energy resolution, and sensitivity values of the gamma camera with the CdZnTe detector and the gamma camera with NaI(Tl) detector are respectively: 7.16 mm, 5.1% and 17.5 cps/µCi for CdZnTe, and 13.2 mm, 9.4% and 3.9 cps/µCi for NaI(Tl) µCi respectively.

Conclusion: According to the results of our study, it was concluded that the energy resolution, spatial resolution, sensitivity, and linearity properties of the gamma camera with the semiconductor CdZnTe detector are superior to those of the gamma camera with the NaI(Tl) detector.

Keywords: Gamma camera, semiconductor detector, CdZnTe, energy resolution, spatial resolution

ÖZ

Amaç: Son yıllarda yarı iletken dedektörlere (CdZnTe) sahip gama kameralar, nükleer tıpta tanısal sintigrafik görüntülemede rutin uygulamaya girmiştir. Bu çalışmasında, yarı iletken dedektörlü (CdZnTe) bir gama kamera ile NaI(Tl) dedektörlü konvansiyonel bir gama kameranın performans özelliklerinin karşılaştırılması amaçlanmıştır.

Gereç ve Yöntemler: Deneysel çalışmalarımızda, farklı aktivitelerde Tc-99m radyoizotopu yerleştirilen aynı uzunluk ve kalınlığa sahip 3 kapiller tüp kullanılarak uzaysal çözünürlük, enerji çözünürlüğü ve doğrusal testler yapılmıştır. Duyarlılık testleri ise 3 cm çapında plastik petri kabına yerleştirilen Tc-99m ile gerçekleştirilmiştir. Kapiler tüplerin ve petri kabının sintigrafik görüntüleri her iki gama kamera ile eşit geometrik koşullar altında alınmıştır. Görüntüler üzerinde ilgi bölgeleri (ROI) çizilmiştir. ROI'deki sayımlara karşılık gelen aktivite miktarı belirlenmiştir.

Bulgular: CdZnTe dedektörlü gama kamera ile NaI(Tl) dedektörlü gama kameranın uzaysal çözünürlük, enerji çözünürlüğü ve duyarlılık değerleri sırasıyla; CdZnTe için 7,16 mm, %5,1 ve 17,5 cps/µCi, NaI(Tl) için ise 13,2 mm, %9,4 ve 3,9 cps/µCi olarak bulunmuştur.

Sonuç: Çalışmamızın sonuçlarına göre, yarı iletken CdZnTe dedektörlü gama kameranın enerji çözünürlüğü, uzaysal çözünürlüğü, duyarlılığı ve doğrusal özelliklerinin NaI(Tl) dedektörlü gama kameraya göre üstün olduğu sonucuna varılmıştır.

Anahtar Kelimeler: Gama kamera, yarı iletken dedektör, CdZnTe, enerji çözünürlüğü, uzaysal çözünürlük

INTRODUCTION

Nuclear medicine is a scientific discipline in which the diagnosis and treatment of diseases are conducted through the administration of radiopharmaceuticals into the body. Distinguishing itself from anatomical imaging systems, its primary advantage lies in providing images that reflect the biological processes of organs at the cellular and molecular levels. Nuclear medicine also encompasses significant complementary methods for conventional radiological imaging. One of the scintigraphic imaging devices used in nuclear medicine is the gamma camera. The more advanced version of these devices, allowing for tomographic imaging, is referred to as Single Photon Emission Computerised Tomography (SPECT) gamma cameras. In evaluating the operational performance of a gamma camera, the homogeneity, linearity, energy resolution, spatial resolution, system sensitivity (or efficiency), and count rate performances are assessed (1, 2).

The primary aim of developing CZT gamma cameras has been to enhance image contrast by achieving better energy resolution while maintaining a spatial resolution comparable to that of scintillation cameras equipped with a low-energy high-resolution (LEHR) collimator, typically yielding 8–9-mm FWHM at a distance of 10 cm from the collimator face, a scenario common in most clinical examinations. In addition to designing the imaging system, automatic handling and assembly methods were developed to ensure detector positioning accuracy and enable cost-effective manufacturing and maintenance in the long term (3).

Following the recognition of the superior characteristics of semiconductor technology in ionising radiation detection, it has also been incorporated into gamma cameras. CdZnTe detector-based gamma cameras have been particularly employed for cardiac scintigraphy, and their usage is progressively expanding in contemporary practise (4).

The spatial resolution performance of the CZT is ultimately constrained by the size of the electron cloud and the diffusion of electrons within it. Resolution refers to the full width at half maximum (FWHM) of the camera's response to full photopeak radiation emitted from a line source positioned with its longitudinal axis aligned along a major axis of the crystal. While other parameters also contribute to describing the resolution, such as

those outlined below, FWHM is commonly used to characterise scanning collimators. It proves valuable in illustrating performance fluctuations concerning differing gamma-ray energies, source-collimator distances, and variations across the crystal's surface (5).

The CZT detector offers a significant advantage in terms of enhanced energy resolution. The determination of energy resolution hinges upon several factors: (a) Electronic noise stemming from the input stage of the preamplifier, inclusive of the capacitance and leakage current inherent to the detector; (b) Linewidth attributed to the stochastic characteristics of charge generation; and (c) Fluctuations arising from the trapping of charge carriers within the detector. Linearity is the characteristic of a gamma camera that dictates its capacity to accurately replicate the spatial distribution of an isotope (6).

Sensitivity is quantified as the proportion of gamma rays that interact within the detector compared to the total number incident upon it. It serves as a crucial determinant of the camera system's efficacy. Inadequate detector design can lead to subpar overall performance (4).

This study aims to compare the performance characteristics of spatial resolution, linearity, energy resolution, and sensitivity between conventional gamma cameras with NaI(Tl) detector material and gamma cameras with the CdZnTe (semiconductor) detector material of the same brand.

MATERIALS AND METHODS

Experimental materials and radionuclide activities

Tc-99m activities were measured using a dose calibrator, and the solutions were prepared in separate vials at concentrations of 1 mCi/5ml, 2 mCi/10ml, and 3 mCi/15ml, respectively. From each vial, Tc-99m solutions were drawn into capillary tubes with internal diameters of 1 mm, lengths of 7.5 cm, and volumes of 0.8 ml. The tube ends were sealed with putty. The activity within the tubes was measured using a dose calibrator, and the net Tc-99m activities were determined after the background count corrections. The measurement times were recorded. The tubes were placed on a cardboard surface with a 4- cm spacing between them and were securely fixed in preparation for imaging.

Gamma cameras and imaging techniques

The experiments were conducted on two different gamma ca-

Table 1: GE Brand Discovery NM 530c Brand CdZnTe Detector and GE Tandem Discovery 630 NaI(Tl) detector gamma camera physical properties

Physical properties	GE discovery NM 530c	GE Tandem discovery 630
Crystal thickness	5 mm	12.4 mm
Detector material	CdZnTe	NaI(Tl)
Gamma camera type	SPECT	SPECT
Collimator type	Pin Hole	Parallel Hole (LEHR)
Detector density	5.78 g/cm³	3.76 g/cm³
Light transformation	100%	13%
Dead time	No	>20000 counts

GE: General Electric, NM: Nuclear Medicine, CdZnTe: Cadmium Zinc Tellure, NaI(Tl): Sodium Iodure (Thallium), SPECT: Single Photon Emission Tomography
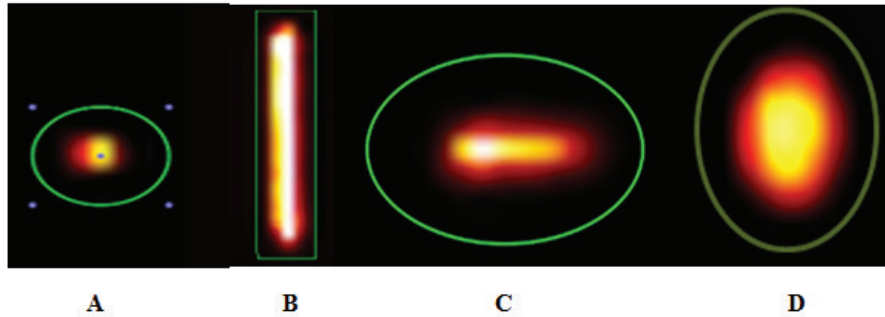
Figure 1: Capillary tube in different planar section images (A) short axis (axial) section (B) long axis (sagittal) section (C) long axis (coronal) section D) petri dish. (outer contours are ROI plots)

meras. One of them is the GE brand, Discovery NM 530c model, with a CdZnTe detector Gamma Camera. The detector assembly consists of a multi-pinhole collimator. Each pinhole in the block illuminates a solid-state pixellated gamma-ray detector made of CZT. Similarly, each pinhole and detector creates a complete miniature gamma camera. The other is the GE brand, Tandem Discovery 630 model, with a NaI(Tl) detector and LEHR collimator gamma camera. The technical specifications of these gamma cameras are provided in Table 1.

The capillary tubes were imaged under identical geometric conditions in two different gamma cameras. The distance between the detector and the tube was kept constant at 18 cm. Image acquisitions were performed based on the total counts according to the clinical imaging procedure. The imaging durations for the Discovery NM 530c and Tandem Discovery 630 devices were 7 min and 6.04 min, respectively.

Image quantifications

Image quantifications were conducted on the gamma camera workstations. Images were transferred to the workstation, and regions of interest (ROIs) were drawn around the tubes. Total counts within the ROIs were determined. Activity loss corrections were applied separately for each capillary tube. Count/activity quantities were determined for each of the three tubes.

Spatial resolutions for gamma cameras were extracted separately for tubes with three different activities. Count variation data between 0 and 40 mm in SPECT axial section images of the tubes were determined. These position-count data were transformed into a Gaussian fit graph using the mathematical formulas below, allowing the calculation of spatial resolutions and energy resolutions (7).

$$Spatial\ resolution, FWHM\ = 2.d.\sqrt{2.ln2}$$

$$Energy\ resolution, FWHM\ \% = \frac{Spatial\ resolution}{Gamma\ Energy\ of\ Radionuclide}\ x100$$

$$FWHM\ \% = \frac{2.d.\sqrt{2.ln2}}{140\ keV}.100$$

The linearity measurements were derived from the count measurements of the capillary tubes with three different activities. Linearity was determined by plotting the count-activity variations of tubes separately imaged and the ROIs drawn in the gamma cameras.

For sensitivity measurements, a 0.5 mCi/3ml Tc-99m solution was placed in a 3 cm diameter plastic Petri dish. The net activity was first measured in the dose calibrator, and the measurement time was recorded. The Petri dish was imaged for a duration of 7 min with a fixed geometry in both gamma cameras. The images were transferred to the workstation, and ROIs were drawn to determine the count/activity (cps/mCi) quantities.

RESULTS

Energy resolution and spatial resolution

The count variations in the axial section (short axis) images of three separate capillary tubes in the Tandem Discovery 630 device were determined by drawing ROIs in the 0-4 mm length region (Figure 1). Counts were transferred to the ImageJ programme, and the position-count variations were subtracted in ImageJ. Gaussian position-count variation graphs were obtained using these graphs. Spatial resolutions (mm) and energy resolutions (%) for each gamma camera were then calculated

Table 2: Spatial Resolution (mm) and percentage Energy Resolution Values of the Tandem Discovery 630 Model Gamma Camera with NaI(Tl) Detector and the GE Brand Discovery NM 530c Model (CdTeZn) Gamma Camera with the Detector

	Tandem Discovery 630				Discovery NM 530c			
	1. Tube	2. Tube	3. Tube	Mean	1. Tube	2. Tube	3. Tube	Mean
Activity (mCi)	1.015	2.08	3.09	2.06	1.015	2.08	3.09	2.06
Spatial resolution (mm)	14.221	12.724	12.683	13.210	6.854	7.267	7.377	7.166
Energy resolution (%)	10.158	9.089	9.060	9.435	4.896	5.191	5.269	5.119

NM: Nuclear Medicine, mCi: millicurie

Table 3: Sensitivity Values of the Discovery NM 530c
Gamma Camera and the Discovery NM 630 Gamma Camera

	Discovery NM 530c	Tandem discovery 630
Activity (µCi)	44	40
Counts (cps)	7760.6	1534.7
Sensitivity (cps/µCi)	17.5	3.9

NM: Nuclear medicine, µCi: microCurie, cps: Count per second

for three different tubes and three different Tc-99m activities. Average values were subsequently obtained. Table 2 provides the spatial resolution (mm) and % energy resolution values for the GE Tandem Discovery 630 model NaI(Tl) detector gamma camera, while Table 3 presents the spatial resolution (mm) and % energy resolution values for the GE Discovery NM 530c model (CdTeZn) detector gamma camera.

Linearity

Variations between the ROI counts of the capillary tubes with three different Tc-99m activities and the measured net activity quantities (µCi) in the dose calibrator were plotted (Figure 2 and Figure 3). In Figure 3, it is observed that the linearity of the semiconductor gamma camera with the CdZnTe detector material perfectly coincides with the x = y (first bisector) line and
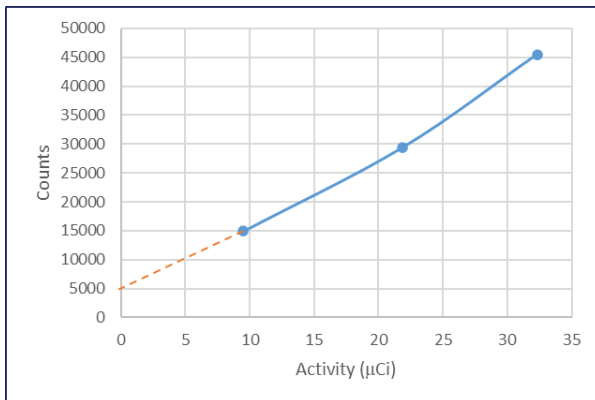

Figure 2: Count-activity linearity graph of the Discovery Tandem 630 model gamma camera
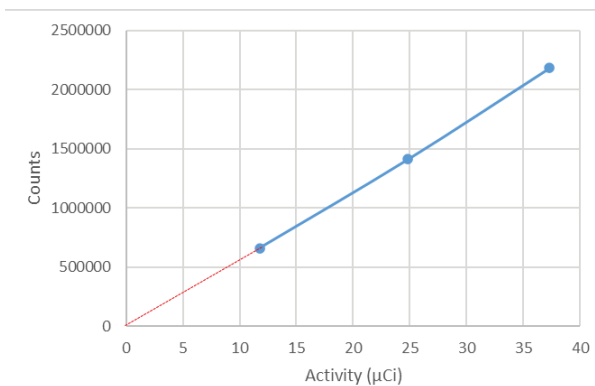

Figure 3: Count-activity linearity graph of the Discovery NM 530c model gamma camera

passes through the origin. The linearity curve of the conventional gamma camera with NaI(Tl) detector material, however, deviates from the origin to some extent, and the linearity is disrupted at count rates >20 cps/µCi.

Sensitivity

The sensitivity values calculated using the petri dish (cps/µCi) for the Discovery NM 530c CdZnTe detector gamma camera are presented in Table 3 and those for the Tandem Discovery 630 NaI(Tl) detector gamma camera are presented in Table 3 The sensitivity values for the Discovery NM 530c and Tandem Discovery 630 gamma cameras were found to be 17.52 cps/µCi and 3.905 cps/µCi, respectively.

DISCUSSION

Semiconductor-based gamma cameras are preferred in nuclear medicine clinics over gamma cameras using NaI(Tl) detector material due to their superior spatial resolution, energy resolution, higher sensitivity, and better linearity. Because of these superior performance characteristics, scintigraphic images of higher quality can be obtained in a shorter time and with lesser number of radiopharmaceuticals. In his study, Barber HB emphasised that semiconductor (CdZnTe) detectors yield good results in terms of spatial resolution and energy resolution in the field of nuclear medicine. He reported that the energy resolution of semiconductor gamma cameras with a CdZnTe detector material is 8% at 140 keV, while conventional gamma cameras with NaI(Tl) detectors have an energy resolution of 11% (8). John K. Hartwell reported an energy resolution of 7.6% for the CZT cameras and 14% for NaI(Tl) detector gamma cameras at 140 keV (9). Oliver Gal et al. found an energy resolution of 4.5% for semiconductor detector gamma cameras and 13% for NaI(Tl) detector gamma cameras at 662 keV (10). Agostini et al. reported an energy resolution of 6% for CZT cameras at 140 keV and 10% for conventional gamma cameras with NaI(Tl) detectors (11). Our results, with an energy resolution of 5.1% for the CdZnTe detector gamma camera and 9.4% for the NaI(Tl) detector gamma camera at 140 keV, are consistent with the literature data.

Analysing recent publications, Hugg et al. reported an energy resolution of 3.6% at 140 keV, a system spatial resolution of 6.8 mm, and a sensitivity of 11.4 cps/µCi for semiconductor CZT cameras (12). When compared to our results, it appears that the spatial resolution, energy resolution, and sensitivity values reported in recent studies are superior. This improvement in the performance parameters may be interpreted as ongoing advancement in the detector and gamma camera technology over time.

The spatial resolution test results investigated by Abe, A. et al. found a system spatial resolution of 2.2 mm at the FOV centre and a sensitivity of 11,052 cpm/MBq (13). In our results, the spatial resolution was 7.16 mm for the CdZnTe detector gamma camera and 13.21 mm for the NaI(Tl) detector gamma camera. Our sensitivity values were 17.518 cps/µCi for the Discovery NM 530c gamma camera and 3.905 cps/µCi for the Discovery

NM 630 gamma camera.

The sensitivity of the CZT camera was assessed in comparison to a 3/8" NaI(Tl) spot crystal Anger camera employing identical geometrical configurations. Energy windows of 6% and 10% were applied to the CZT and NaI detectors, respectively. The sensitivity of the CZT camera was determined to be 70% of that of the 3/8" NaI camera. This implies that approximately 60% of the incident 140 keV gamma photons were detected within the photopeak in the CZT (14). According to our results, the sensitivity of the semiconductor gamma camera was determined to be 77.5% better than that of the NaI(Tl) detector gamma camera.

When the response variations of gamma cameras to activity increases (linearity) were examined; it was found that in Figure 2, when sensitivity is >20 cps/μCi, linearity is disrupted due to the dead time related to the activity increase. In contrast, it was observed that the linearity of the CdZnTe detector gamma camera perfectly coincides with the x=y (first bisector) line and passes through the origin. Additionally, no linearity disruption due to the activity increase was observed in the examined range. This indicates that the linearity of the semiconductor detector gamma camera is more stable.

In addition to the advantages of semiconductor detectors, there are some disadvantages. One of the most significant is their limited field of view (FOV), making them unsuitable for scintigraphic imaging of organs other than the heart due to their small FOV. Nowadays, wider FOV semiconductor detector gamma cameras are also used. However, their high prices are a disadvantage for cameras with semiconductor detectors.

CONCLUSION

In this study, the technical performance of two gamma cameras based on different technologies from the same manufacturer was experimentally measured. According to our results, the sensitivity of the CdZnTe camera was found to be 4.48 times higher than that of the other camera. Consequently, it would be possible to reduce the amount of Tc-99m activity used in myocardial perfusion scintigraphy by the same factor. It was determined that using the CdZnTe camera for myocardial perfusion scintigraphy would reduce the patient's radiation dose by a factor of 4.48. Additionally, the study demonstrated that the radiation exposure to the personnel performing the procedure would decrease, the cost of radiopharmaceuticals would be reduced, and the number of procedures performed daily could be significantly increased.

REFERENCES

1. National Electrical Manufacturers Association. Performance Measurements of Gamma Cameras NEMA NU 1-2018. Rosslyn, VA: National Electrical Manufacturers Association. https://www.nema.org/docs/default-source/standards-document-library/nema_nu_1_2018-contents-and-scope.pdf?sfvrsn=d93985ea_1

2. Koppert WJ, Dietze MM, Van der Velden S, Steenbergen JL, De Jong HW. A comparative study of NaI (Tl), CeBr3, and CZT for use in a real-time simultaneous nuclear and fluoroscopic dual-layer detector. Physics in Medicine & Biology 2019;64(13):135012.

3. Verger L, Gentet MC, Gerfault L, Guillemaud R, Mestais C, Monnet O, et al. Performance and perspectives of a CdZnTe-based gamma camera for medical imaging. IEEE Transactions on Nuclear Science 2004;51(6):3111-7.

4. Amrami R, Shani G, Hefetz Y, Blevis I, Pansky A. A comparison between the performance of a pixellated CdZnTe based gamma camera and Anger NaI (TI) scintillator gamma camera. In Proceedings of the 22nd Annual International Conference of the IEEE Engineering in Medicine and Biology Society. 2000;1:352-5.

5. Zheng X, Cheng Z, Deen MJ, Peng H. Improving the spatial resolution in CZT detectors using charge sharing effect and transient signal analysis: Simulation study. NIMA 2016;808:60-70.

6. Montémont G, Lux S, Monnet O, Stanchina S, Verger L. Studying spatial resolution of CZT detectors using sub-pixel positioning for SPECT. IEEE Transactions on Nuclear Science 2014;61(5):2559-66.

7. Coman E, Brewster MW, Popuri SK, Andrew MR, Matthias KG. A comparative evaluation of Matlab, Octave, FreeMat, Scilab, R, and IDL on Tara. 2012 Oct. Technical Report HPCF–2012–15.

8. Barber H B. Applications of semiconductor detectors to nuclear medicine. NIMA 1999;436(1-2):102-10.

9. Agostinelli S, Allison J, Amako K, Apostolakis J, Araujo H, Arce P, et al. A comparative evaluation of Matlab, Octave, FreeMat, Scilab, R, and IDL on Tara. NIMA 2003;506:250-303.

10. Gal O, Gmar M, Ivanov OP, Laine F, Lamadie F, Le Goaller C, et al. Development of a portable gamma camera with coded aperture, nuclear instruments and methods in physics research section a: accelerators, spectrometers, detectors and associated equipment. NIMA 2006;563(1):233-7.

11. Agostini D, Marie PY, Ben-Haim S, Rouzet F, Songy B, Giordano A, et al. Performance of cardiac cadmium-zinc-telluride gamma camera imaging in coronary artery disease: A review from the Cardiovascular Committee of the European Association of Nuclear Medicine (EANM). EJNMMI 2016;43(13):2423-32.

12. Hugg J, Harris B, Tomita H. Evaluation of CZT Gamma Cameras for Human SPECT and Small FOV Imaging. J Nuclear Med 2018;59(supplement 1):220.

13. Abe A, Takahashi N, Lee J, Oka T, Shizukuishi K, Kikuchi T, et al. Performance evaluation of a hand-held, semiconductor (CdZnTe)-based gamma camera. Eur J Nuclear Med Molecular Imaging 2003;30(6):805-11.

14. Wagenaar D J, Parnham K, Sundal B, Maehlum G, Chowdhury S, Meier D, et al. Advantages of semiconductor CZT for medical imaging. In Penetrating Radiation Systems and Applications 2007;6707:144-53.